

PROCESSING FLY ASH FROM THE THERMAL POWER STATIONS FOR GAS EMISSIONS PURIFICATION FROM SULFUR DIOXIDE

V. S. YEMELYANOVA¹, B. T. DOSSUMOVA², T. V. SHAKIYEVA³,
L. R. SASSYKOVA⁴ & S. SENDILVELAN⁵

^{1,2,3}Scientific and Production Technical Center “Zhalyln” LLP, Almaty, Kazakhstan

⁴Al-Farabi Kazakh National University Almaty, Kazakhstan

⁵Department of Mechanical Engineering, Dr. M. G. R Educational and Research Institute,
University, Chennai, Tamil Nadu, India

ABSTRACT

The aim of the work is development of technology of adsorptive, catalytical- chemisorptive purification of gas emissions from sulfur dioxide with simultaneous separation of sulfonic acids and sulfoxides as reaction products. For this research, the fractions of non-perforated cenospheres from the combustion of coal of Ekibastuz field (Kazakhstan) at the Almaty TPP-2 (Kazakhstan) have been applied. The method of microspherical sorbent obtaining from technogenic aluminosilicate raw material – energetic ash of Almaty TPP-2 has been elaborated. The aluminosilicate composite was studied after modification in the process of SO₂ oxidation by the oxygen in stationary conditions in aqueous solution, in the kinetic mode and in the temperature range of 40-60°C. The conditions of selective oxidation of SO₂ (100 %) to give the sulfuric acid as a product were optimized. The catalysts elaborated were tested in the process of treatment of gases from SO₂ at a pilot vortex stirrer on the model gas mixtures SO₂-Ar with a content of SO₂ up to 1.0 % vol. The results obtained have demonstrated that degree of SO₂ removal reached 87-95%. The structure and composition of the obtained microspherical composite is studied. The iron nanostructural distribution in aluminosilicate is proved with the help of different research methods: IR- and EPR-spectroscopy, X-ray diffraction, SEM, elemental and Chemical analysis.

KEYWORDS: Fly Ash from TPP, Sulphur Dioxide, Microspheres, Gas emissions & Purification

Received: Jun 07, 2019; **Accepted:** Jun 27, 2019; **Published:** Jul 15, 2019; **Paper Id.:** IJMPERDAUG2019105

1. INTRODUCTION

The development of fuel and energy complex envisages substantial growth of a share of production of electrical energy at the cost of solid fuel burning at the thermal power plant (TPP), that necessarily will lead to formation and accumulation of the significant mass of wastes of ash and slag (Vuthaluru et al., 1996; Gupta, et al., 2007; Tulepov et al., 2019; Sassykova et al., 2019). From solid fuel burning at the TPP, it is annually appeared over 100 million ton of bottom-ash wastes which are accumulated in dumps. The total area of the land occupied under dumps compounds ca. 35,000 hectares (Rubio et al., 2010; Tashmukhambetova et al., 2017; Ponomarenko et al., 2017). Over 1.5 billion tons of bottom-ash wastes are warehoused at the TPP ash dumps, and the level of their use compounds 10-15 % that is significant below than use level in the developed countries. In this connection, the problem of a utilization of ash and slag of the TPP working on solid fuel is very actual. Results of our researches (Kairbekov et al., 2015; Yemelyanova et al., 2015; Zaripova et al., 2015; Yemelyanova et al., 2013), in Kazakhstan (Sassykova et al., 2018; Baiseitov et al., 2017; Tukhtin et al., 2019; Rakhimova et al., 2017) and abroad (Prokopenko, et

al., 2016; Sasi, T., et al., 2018; Vereshchagina et al., 2004; Anshits et al., 2001; Zinoviev et al., 2016; Fomenko et al., 1998; Abotsi et al., 1996) demonstrated that a row of the components possessing valuable, in many cases unique technological properties, allow using them effectively in many modern technology contains in fly ash of TPP. These are aluminosilicate hollow microspheres (AHM), magnetite microbeads, the unburnt carbonic particles, ferrosilicon and carbonate microspheres (Maloletnev et al., 2015; Gabdrashova et al., 2018; Tulepov et al., 2018). AHM are formed as a part of fly ash at coals burning as a result of fusion of mineral components, the subsequent granulation of a melt on separate smallest drips in a gas stream and its inflation for the account of gaseous inclusions volume augmentation. The main component of ash and slag is silicon oxide SiO_2 (45-60%), followed by alumina Al_2O_3 (15-25%), iron oxides Fe_2O_3 (5-15%), calcium oxide CaO (1.5-4.5%), potassium oxide K_2O (2.0-4.5%) and some other oxides, the content of which usually does not exceed 1%. Thanks to the correct spherical shape and low density microspheres possess properties of perfect filler in the most diverse products. In terms of their properties, AHM from ash of coal TPP are close to the hollow microspheres made by special industrial methods from melts of natural or artificial materials, and used in the quality of excipients of various composite materials (Maloletnev et al., 2013; Wang et al., 2002; Baiseitov et al., 2016). However, scales of production of hollow microspheres are restricted because of the complicated technology and the high cost. The cost of hollow microspheres separated from ash with industrial expedients is significant below than industrial, and their “production” at the TPP is valued by tens thousand tons a year.

Ash dumps of coal combined heat and power plants can be considered as deposits, if it or the components containing in it are suitable for economically feasible and environmentally safe industrial use. The material of ash dumps (“mineral wealth”) for all these characteristics should not be inferior to the traditionally used raw materials, and its development – have to justify investment in the organization of producing (Itoh et al., 1984; Aubakirov et al., 2017; Tanimoto et al., 1998). The organization of large-scale extraction and widespread introduction into the production of AHM, magnetite microbeads are hampered by the lack of systematic data on their composition, physical and technological properties.

The aim of the work was to elaborate the technology of adsorptive, catalytical-chemisorptive purification of gas emissions from sulfur dioxide with simultaneous separation of sulfonic acids and sulfoxides as reaction products by using. For this research, the fractions of non-perforated cenospheres from the combustion of coal of Ekibastuz field (Kazakhstan) at the Almaty TPP-2 (Kazakhstan) have been applied.

2. EXPERIMENTAL

Fractions of non-perforated cenospheres from the combustion of coal of Ekibastuz field (Kazakhstan) at the Almaty TPP-2 (Kazakhstan) with an aluminosilicate module $\text{SiO}_2/\text{Al}_2\text{O}_3 = 3.2$ and an iron content of 3.03-3.67 wt.% in Fe_2O_3 (Table 1) have been applied. Such a composition of the cenospheres is preferable for the crystallization of zeolite NaP with a gismondine type framework. Ekibastuz coal basin on the territory of Kazakhstan is one of the most significant by reserves and ranks first in the world in terms of coal density: on the area of 62 square kilometres, the coal reserves are estimated at 13 billion tons or 200 tons per square meter. It is one of the most promising coal basin in the world by open-pit coal mining (Tulepov et al., 2019). The main consumers of coal from this basin are in the Urals and in the Republic of Kazakhstan.

The Figure 1 shows the external appearance and wall cross-section of the non-perforated cenospheres of the - 0.18+0.08 mm fraction.

Table 1: Properties of Cenospheres Fractions, used for Research

Sample	Fraction, mm	Macrocomponent Composition, wt. %			SiO ₂ /Al ₂ O ₃ , wt %	Crystalline phase, wt. %			Glass phase	S _{BET} , m ² /g
		SiO ₂	Al ₂ O ₃	Fe ₂ O ₃		quartz	mullite	calcite		
T-3.2	-0.18+0.08	67.60	20.95	3.03	3.2	3.4	0.8	0.5	95.4	125
H-3.2	-0.18+0.08	66.50	20.71	3.67	3.2	n. d.*	n. d.*	n. d.*	n. d.*	125

*n. d. – not determined

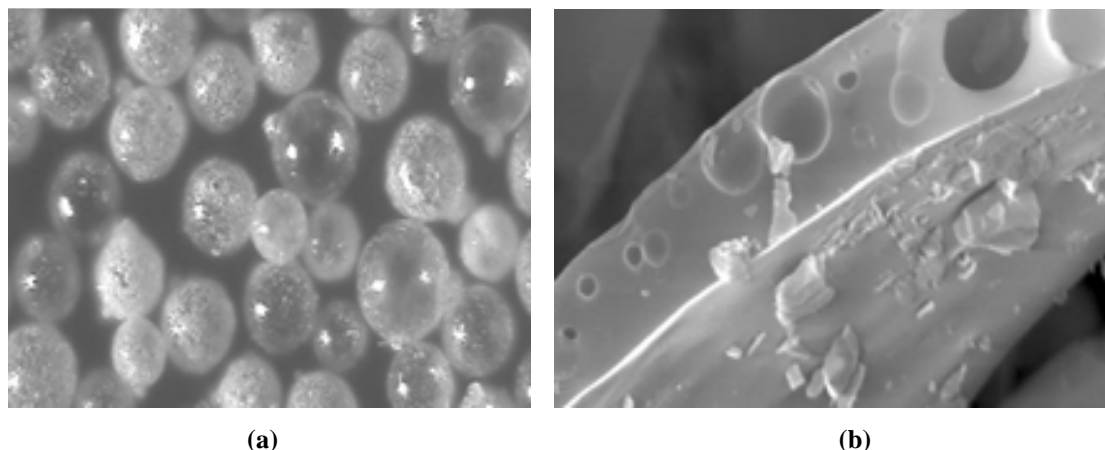


Figure 1: External Appearance (a) and Cross-Section (b) of the Fraction Wall of the Non-Perforated Cenosphere -0.18+0.08 mm (Sample T-3.2)

The Table 2 summarizes the optimal results of the production of zeolites on the basis of cenospheres and their phase composition of the obtained zeolites.

Table 2: Effect of the Processing Conditions on the Process of Zeolitization of the Cenospheres in the Static Conditions

No of a sample	t, °C	C _{NaOH} , mol/l	τ, hour	S _{sp} , m ² /g	Phase composition
1	32	-	-	-	Amorphous glass phase, quartz
2	45	2.5	72	1.2	Amorphous glass phase, quartz
3	80	4.4	80	194	NaX, NaA, NaP1
4	100	1.0	72	37	NaP1
5	100	2.5	72	63	NaX, NaP1
6	180	1.0	24	58	NaP1

In this work, the phase composition of aluminosilicate microspheres (cenospheres) was determined using the Rietveld refinement on a powder x-Ray diffractometer Ultima IV (Rigaki) with a solid-state detector and two-position graphite monochromator for CuK α radiation ($\lambda = 0.15406$ nm), generator power – 40 kV and 40 mA, measurement interval (2 θ); 10-70°, scanning speed – 4° min⁻¹. The cenospheres shell structure was studied using a Scanning Electron Microscope of Hitachi High-Technologies Corporation, S-2400 with an accelerating voltage 15 kV. The cenospheres specific surface area was calculated from the total isotherms of low-temperature nitrogen adsorption by the BET method measured on the device Bell SORP (Bell Japan Inc.). Elemental and chemical analysis was performed using an x-ray fluorescence spectrometer Thermo Fisher Scientific K/K/ Flash EA1112.

The kinetics of oxidation of sodium sulfite with oxygen was studied in the stationary conditions using a glass non-gradient thermostatic reactor of the “duck” type equipped with a potentiometric device. The kinetic mode was provided by intensive shaking of the reactor (300-400 swings per min.), the volume of the liquid phase was not more than 40 cm³, with a total reactor volume 180 cm³. The reaction rate was monitored by the oxygen absorption from the thermostatic burette

connected to the reactor. For the classification of fly ash from coal combustion, a column pulsation apparatus with pneumatic pulsators and swirling partitions has been applied in the experiments. The distance between the partitions was 80 mm, and the cross-section wet area of the ajutage was 30 %. The rate of upward flow of the water was 0.005 m/s, an amplitude of pulsation was kept within 5 mm. The pulsations frequency was varied within the relationships density/specific surface area which are inherent to the two non-magnetic products (quartz sand and $\gamma\text{-Al}_2\text{O}_3$). In this case 0.2-5.0 imp./min. at the bottom of the column there is an annular electromagnet providing the required range of magnetic field intensity in the upstream section (1,000 G). The efficiency of the process was evaluated by the results of X-ray phase analysis and by means of visual control of quality of the selected products using a microscope.

The fly ash suspension was introduced through the funnel to the level of 0.1; 0.2; 1.0; 1.5; 1.6 m in height of the upward flow. The flushing water was supplied through the lower tubulure of the column apparatus in the zone of the pulsation chamber. The output of hollow microspheres was determined after deposition of the suspension of column upper discharge in the sump. Depending on the input level of the initial suspension, the output of hollow microspheres was 51, 82, 84, 88, 89 and 88 %, respectively.

To study the kinetics of oxidation of sulfur dioxide by oxygen in stationary conditions in the presence of modified cenospheres as a catalyst, Na_2SO_3 was used as a source of SO_2 , because under the experiment conditions at pH =10-12 in an aqueous solution SO_2 is in the form of SO_3^{2-} and the reaction (1) was actually studied



For magnetic measurements, a vibration magnetometer AMH-500 Hysteresisograph (Italy) was used, and electron microscopic studies and electron probe analysis were performed using the Camebax-Microbeam instrument (France), the phase composition was monitored by X-ray analysis using the Dron-0.5 X-ray diffractometer, the chemical composition of the catalyst surface was studied using the ES-2401 X-ray photoelectron spectrometer, and the chemical composition of the surface was studied using the Auger spectrometer pH1-590. The physical and chemical features of magnetic polymer composites were studied using the modern methods of analysis according to the common techniques (Hamasaki et al., 2008; Bhaskar et al., 2018; Sassykova et al., 2017; Lanzerstorfer, 2018; Lu et al., 2006).

3. RESULTS AND DISCUSSIONS

The main results of the study of microspherical catalysts of oxidation of sodium sulfite by oxygen are summarized in the Table 3.

Table 3: Oxidation of Sodium Sulfite by Oxygen in the Presence of a Microspherical Catalyst at T=40°C

No of the Test	Ash weight, g	Concentration, mole/l			Na_2SO_3 Conversion degree, %	W_{O_2} , max, ml/min
		Na_2SO_3	FeSO_4	H_2SO_4		
1	0	0.4	-	-	100.0	0.6
2	0.1	0.4	-	-	100.0	5.4
3	0.5	0.4	-	-	100.0	4.4
4	1.0	0.4	-	-	100.0	4.0
5	2.0	0.4	-	-	-	3.4
6	0.1	0.2	-	-	100.0	4.8
7	0.1	0.1	-	-	100.0	3.6
8	0.1	0.2	$1 \cdot 10^{-4}$	-	100.0	4.0
9	0.1	0.2	$0.5 \cdot 10^{-5}$	-	100.0	4.6
10	0.1	0.2	$1 \cdot 10^{-5}$	-	100.0	6.8
11	0.1	0.2	10^{-2}	-	79.0	3.8

Table 3: Contd.,						
12	0.1	0.2	-	-	100.0	4.8
13	0.1	0.2	-	$1.75 \cdot 10^{-2}$	100.0	5.2
14	0.1	0.2	-	$5.2 \cdot 10^{-2}$	100.0	3.8
15	0.1	0.2	-	$8.75 \cdot 10^{-2}$	100.0	3.0

The results of the Table 3 showed that the degree of conversion and the ratio of the process depended on the concentrations of components of the system $\text{Na}_2\text{SO}_3 - \text{Al}-\text{O}-\text{Si}-\text{Fe} - \text{H}_2\text{SO}_4 - \text{H}_2\text{O}$. Under optimal conditions, the Na_2SO_3 rate conversion reaches 100 %, the maximum oxygen absorption rate reaches 6.8 ml/min. In most cases, the Na_2SO_3 oxidation rate dependence on the initial concentrations of the components has extreme nature (Figures 2, 3).

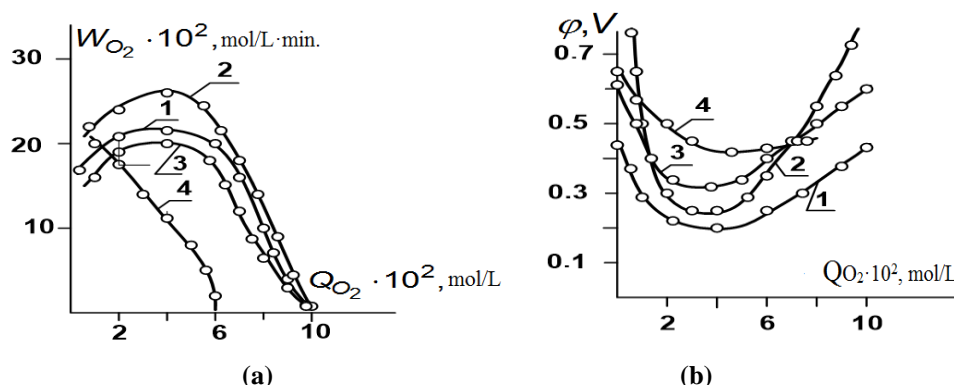


Figure 2: Oxidation of Sodium Sulfite by Oxygen in the presence of Microspherical Alumino Silicates at $T = 313\text{K}$, $P_{\text{O}_2} = 0.1 \text{ MPa}$; Concentration: $\text{Na}_2\text{SO}_3 = 0.2 \text{ mole/L}$, $\text{H}_2\text{SO}_4 = 10^2 \text{ mole/L}$: 1 – 1.75; 2 – 3.50; 3 – 5.25; 4 – 7.0

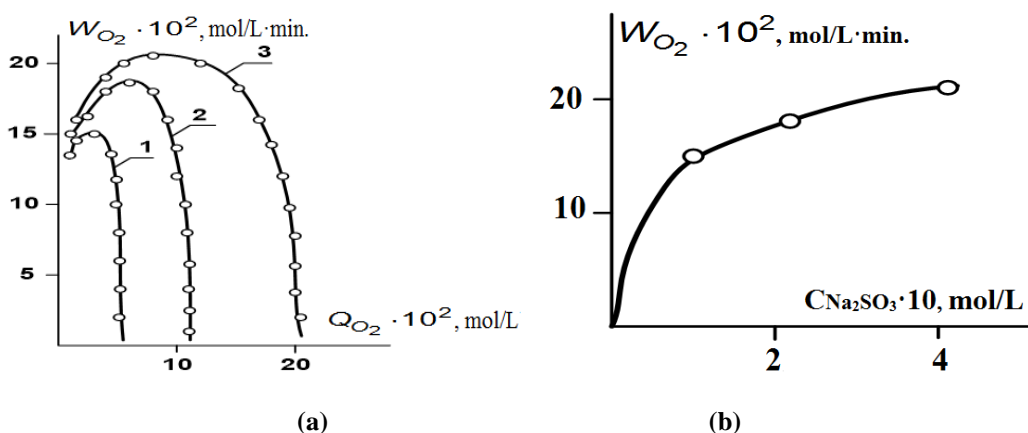


Figure 3: Oxidation of Sodium Sulfite by Oxygen in the Presence of Microspherical Alumino Silicates at $T = 313\text{K}$, $P_{\text{O}_2} = 0.1 \text{ MPa}$; Concentration: $\text{Na}_2\text{SO}_3 = 1 - 0.1$; 2 – 0.2; 3 – 0.4 mole/L

Typical conversion curves in coordinates $W_{\text{O}_2} = f(Q_{\text{O}_2})$, where W_{O_2} is the rate of oxygen absorption in mol/l·min; Q_{O_2} is the amount of absorbed oxygen in mole/l, as well as potentiometric curves in coordinates $\varphi(Q_{\text{O}_2})$, where $\varphi(\text{V})$ is the redox potential of the platinum electrode in relation to the calomel half-element are shown in Figures 2,3. The initial redox potential of the $\text{Na}_2\text{SO}_3 - \text{Al}-\text{O}-\text{Si}-\text{Fe}-\text{MX}-\text{H}_2\text{SO}_4 - \text{H}_2\text{O}$ system, where MX is a modifying component, is placed in the range 0.8–0.45 V, with $d\varphi/C_{\text{Na}_2\text{SO}_3} < 0$, passing through the maximum, $d\varphi/dT > 0$. These results allow to suppose that the redox-determinative pair in this case is $\text{Fe}^{3+}/\text{Fe}^{2+}$. Conversion curves in coordinates $W_{\text{O}_2} = f(Q_{\text{O}_2})$ (Figures 2a, 3a) and potentiometric curves in coordinates $\varphi = f(Q_{\text{O}_2})$ (Figure 2b) show that with the Na_2SO_3 introduction into the redox system,

the potential sharply shifted to the cathode region by 0.5-0.25V, and oxygen absorption starts immediately. The potential jump depends on the components correlation in the system. In the course of the experiment, the potential returns to the anode region, in optimal conditions – to the initial value, which indicates that the reaction products do not change the structure and composition of the catalyst, and it works stably under these conditions. In these conditions, the potential remains at a certain value, without returning to the original value, and for these conditions (Figure 2a, curve 4), the violation of the stoichiometry of the reaction (1) is observed. The conversion curves obtained by varying in the range from 0.11 to 0.4 mol/l are presented in the Figure 3a. The linear dependence between the amount of absorbed oxygen and the initial concentration of Na_2SO_3 is observed in the studied range of sodium sulfate concentrations.

The correlation $C_{\text{Na}_2\text{SO}_3}/Q_{\text{O}_2}=2$ and the correspondence of the stoichiometry of the reaction (1) are preserved throughout the studied interval. The dependence (Figure 3b) of the oxygen absorption rate (Q_{O_2} at $Q_{\text{O}_2} = 1/2$ from ΣQ_{O_2}) is described by the equation (2):

$$W_{\text{O}_2}=(k_1 \cdot \beta_1 \cdot C_{\text{Na}_2\text{SO}_3})/(1+ \beta_1 \cdot C_{\text{Na}_2\text{SO}_3}) \quad (2)$$

where, β is the constant of Na_2SO_3 adsorption on the surface of aluminosilicate microspheres. The data of the Table 3 also indicate on the Na_2SO_3 sorption.

The developed catalyst has been tested in the process of treatment of gases from SO_2 at a pilot vortex stirrer of design capacity 2 m³/h on model gas mixtures SO_2 –Ar containing up to 1 % vol. of SO_2 . Obtained results have demonstrated that with gas feed speed of 10,000-15,000 h⁻¹ degree of removal of SO_2 reaches 87-95 %.

With the help of modern physico-chemical methods, composition and structure of ashes of TPP have been studied. Optimum sizes of active parts of the catalyst are 40-50 nm. Specific surface of the catalyst calculated according to full isotherms of low-temperature adsorption of nitrogen by BET method makes 12.6 m²/g. Integral volume of pores makes 0.57 ml/g.

Thus, a catalytic method of sulfur compounds oxidation by oxygen in an aqueous solution at a temperature range of 0-80°C has been developed. Detailed studies of the process kinetics have shown that as a result, the water-soluble sulfoacids that are good flotation agents, surface-active substances and repellents are formed in solution. Multiple circulation of the aqueous solution makes it possible to obtain 60-70% solution of sulfoacids in the form of a commercial product.

4. CONCLUSIONS

- A method of obtaining a microspherical sorbent from technogenic aluminosilicate raw material - energy ash of Almaty TPP-2 was developed.
- A technological scheme for separating concentrates of cenospheres with obtaining narrow fractions of cenospheres of constant composition with a given size, morphology and magnetic properties has been elaborated. The methods of directional modification of cenospheres with the purpose of obtaining microspherical sorbents of various modifications in a magnetic field and without it are determined.
- Results of the experiment performed demonstrated that microspheres of fly ash are highly effective sorbents of SO_2 and low-temperature catalysts of oxidation of Na_2SO_3 with oxygen in water solutions. At gas feed speed of 10,000-15,000 h⁻¹ degree of removal of SO_2 reaches 87-95 %.

- The optimum sizes of active parts of the catalyst were equal to 40-50 nm. Specific surface of the catalyst calculated according to full isotherms of low-temperature adsorption of nitrogen by BET method makes 12.6 m²/g. Integral volume of pores makes 0.57 ml/g.

REFERENCES

1. Vuthaluru, H. B., Domazetis, G., Wall, T. F. & Vleeskens, J. M. (1996). Reducing fly ash deposition by pretreatment of brown coal: Effect of aluminium on ash character, *Fuel Processing Technology*, 46(2), 117-132. [https://doi.org/10.1016/0378-3820\(95\)00051-8](https://doi.org/10.1016/0378-3820(95)00051-8).
2. Gupta, S. K., Wall, T. F., Creelman, R. A. & Gupta, R. P. (2007). Thermo mechanical analysis of laboratory ash, combustion ash and deposits from coal combustion, *Fuel Processing Technology*, 88(11-12), 1099-1107. <https://doi.org/10.1016/j.fuproc.2007.06.028>.
3. Tulepov, M., Mansurov, Z., Sassykova, L., Baiseitov, D., Dalehanuly, O., Ualiev, Zh., Gabdrashova, Sh. & Kudyarova, Zh. (2019). Research of iron-containing concentrates of Balkhash deposit (Kazakhstan) for processing of low-grade coal, *Journal of Chemical Technology and Metallurgy*, 54(3), 531-538.
4. Sassykova, L. R., Sendilvelan, S., Bhaskar, K., Zhumakanova, A. S., Aubakirov, Y. A., Abildin, T. S., Kubekova, Sh. N., Mataeva, Z. T. & Zhakupova, A. A. (2019). Norms of emissions of harmful substances generated from vehicles in the different countries of the world, *News of the National Academy of Sciences of the Republic of Kazakhstan, series of geology and technology sciences*, 434 (2), 181-189. <https://doi.org/10.32014/2019.2518-170X.53>.
5. Rubio, B. & Izquierdo, M. T. (2010). Coal fly ash based carbons for SO₂ removal from flue gases, *Waste Management*, 30(7), 1341-1347.
6. Tashmukhambetova, Zh., Aubakirov, Y., Shomanova, Zh., Burkhanbekov, K., Safarov, R., Sassykova, L., Zhakirova, N. & Faizullaeva, M. (2017). The effects of pretreatment methods of carbon-containing wastes in thermal catalytic recycling, *Oriental Journal of Chemistry*, 33(6), 2884-2890. <http://dx.doi.org/10.13005/ojc/330622>.
7. Ponomarenko, O., Matveyeva, I., Beisembayeva, L. & Romanova, S. (2017). Effective methods of purification of exhaust gases of TPP from sulfur-containing compounds, *International Multidisciplinary Scientific GeoConference Surveying Geology and Mining Ecology Management, SGEM*, 17(51), 353-358.
8. Yemelyanova, V. S., Kurokawa, H., Dossumova, B. T., Kairbekov, Zh. K., Shakiyeva, T. V., Myltykbaeva, Zh. K., Dzhatkambayeva, U. N., Shakiyev, E. M. & Aybasov, E. Zh. (2015). Using of microspheres of power ashes for gases cleaning from sulphur dioxide, *Advanced Materials Research*, 1079-1080, 110-117. <https://doi.org/10.4028/www.scientific.net/AMR.1079-1080.110>.
9. Yemelyanova, V. S., Shakieva, T. V., Kairbekov, Zh. K., E. M. Shakiev & Baizhomartov, B. B. (2013). Low-temperature catalytic clearing of gases of thermal power station from harmful impurity in the presence of the cobalt complexes fixed on a polymeric matrix, *Advanced Materials Research*, 807-809, 1586-1592. <https://doi.org/10.4028/www.scientific.net/AMR.807-809.1586>.
10. Sassykova, L. & Nalibayeva, A. (2018). Development and testing of catalysts on metal block carriers for exhaust gases neutralization, *Journal of Chemical Technology and Metallurgy*, 53(2), 289-295.
11. Rakhimova, A., Abilzhan Khussainov, A., Grinfelde, I. (2017). Impact of coal ash and phosphogypsum application on soil fertility of Chernozem soils of North Kazakhstan. <https://doi.org/10.22616/erdev2017.16.n220>

12. Prokopev, S. A., Chanturiya, V. A., Bolotin, M. L., Shulgina, M. Ye. & Prokopev, Y. S. (2016). Complex processing of ash and slag wastes from coal-fired CHP plants. In: Litvinenko V. (eds) XVIII International Coal Preparation Congress. Springer, Cham. https://doi.org/10.1007/978-3-319-40943-6_52.
13. Sasi, T., Mighani, M., Örs, E., Tawani, R. & Martin Gräbner (2018). Prediction of ash fusion behavior from coal ash composition for entrained-flow gasification, *Fuel Processing Technology*, 176, 64-75. <https://doi.org/10.1016/j.fuproc.2018.03.018>.
14. Vereshchagina, T. A., Anshits, N. N., Maksimov, N. G., Vereshchagin, S. N., Bayukov, O. A. & Anshits, A. G. (2004). The Nature and Properties of Iron-Containing Nanoparticles Dispersed in an Aluminosilicate Matrix of Cenospheres, *Glass Physics and Chemistry*, 30(3), 247-256.
15. Anshits, A. G., Kondratenko, E. V., Fomenko, E. V., Kovalev, A. M., Anshits, N. N., Bajukov, O. A., Sokol, E. V. & Salanov, A. N. (2001). Novel glass crystal catalysts for the processes of methane oxidation, *Catalysis Today*, 64(1-2), 59-67.
16. Zinoviev, V. N., Kazanin, I. V., Pak, A. Yu., Vereshchagin, A. S., Lebiga, V. A. & Fomin, V. M. (2016). Permeability of Hollow Microspherical Membranes to Helium, *Journal of Engineering Physics and Thermophysics*, 89(1), 25-37.
17. Fomenko, E. V., Kondratenko, E. V., Salanov, A. N., Bajukov, O. A., Talyshev, A. A., Maksimov, N. G., Nizov, V. A. & Anshits, A. G. (1998). Novel Microdesign of Oxidation Catalysts: Part 1. Glass Crystal Microspheres as New Catalysts for the Oxidative Conversion of Methane, *Catalysis Today*, 42(3), 267-272.
18. Abotsi, G. M., Bota, K. B., Saha, G. & Mayes, S. (1996). Effects of surface active agents on molybdenum adsorption onto coal for liquefaction, *Prepr. Pap.-Am. Chem. Soc., Div. Fuel Chem.*, 41, 984-987.
19. Maloletnev, A. S., Mazneva, O. A. & Naumov, K. I. (2015). Mechanochemical activation of coal from the Erkovetskoe deposit and its reactivity in a liquefaction process, *Solid Fuel Chemistry*, 49(6), 372.
20. Gabdrashova, Sh. E., Rakhova, N. M., Pustovalov, I. O., Elemesova, Zh., Tulepov, M. I., Korchagin, M. A., Sassykova, L. R., Sendilvelan, S. & Baiseitov, D. A. (2018). Preparation of mechanically activated mixtures of titanium with the carbon nanotubes and study of their properties under thermal explosion, *Rasayan J. Chem.*, 11(1), 324-330. <http://dx.doi.org/10.7324/RJC.2018.1112017>
21. Maloletnev, A. S. & Gyl'maliev, A. M. (2013). Structure of coal hydrogenation products obtained in the presence of oil and coal paste-forming agents, *Solid Fuel Chemistry*, 47(4), 231.
22. Wang, Q. M., Shen, D., Bulow, M., Lau, M. L., Deng, Sh., Fitch, F. R., Lemocoff, N. O. & Semanscin, J. (2002). Metallo-organic molecular sieve for gas separation and purification, *Microporous and Mesoporous Mater.: Zeolites, Clays, Carbons and Related Materials*, 2, 217. [http://dx.doi.org/10.1016/s1387-1811\(02\)00405-5](http://dx.doi.org/10.1016/s1387-1811(02)00405-5).
23. Itoh, H., Hidalgo, C. V., Hattori, T., Niwa, M. & Murakami, Y. J. (1984). Role of acid property of various zeolites in the methanol conversion to hydrocarbons, *Journal of Catalysis*, 85(2), 521-526.
24. Tanimoto, Y., Tanaka, H., Fujiwara, Y. & Fujiwara, M. (1998). Effects of high magnetic field on the lifetime of chain-linked triplet biradicals composed of xanthone ketyl and xanthenyl radicals, *J. Phys. Chem. A*, 102 (28), 5611-5615.
25. Hamasaki, A., Yago, T. & Wakasa, M. (2008). Magnetic Field Effect on a Radical Pair Reaction as a Probe of Microviscosity, *J. Phys. Chem. B*, 112 (45), 14185-14192.
26. Bhaskar, K., Sassykova, L. R., Prabhakar, M. & Sendilvelan, S. (2018). Effect of dimethoxy-methane (C₃H₈O₂) additive on emission characteristics of a diesel engine fueled with biodiesel, *International Journal of Mechanical and Production Engineering Research and Development*, 8(1), 399-406.

27. Lanzerstorfer, C. (2018). Pre-processing of coal combustion fly ash by classification for enrichment of rare earth elements, *Energy Reports*, 4, 660-663. <https://doi.org/10.1016/j.egyr.2018.10.010>.
28. Lu, G., Yan, Y., Colechin, M. & Hill, R. (2006). Monitoring of oscillatory characteristics of pulverized coal flames through image processing and spectral analysis, *IEEE Transactions on Instrumentation and Measurement*, 1, 55. <http://dx.doi.org/10.1109/TIM.2005.861254>.

